

# Supporting Information for Promising anode materials for alkali metal ion batteries: A case study on cobalt anti-MXenes

Subhadeep Banerjee,<sup>1,2</sup> Ankita Narwal,<sup>1,3</sup> Sandeep K Reddy,<sup>5</sup> and Sharma S. R. K. C. Yamijala<sup>1,2,3,5,\*</sup>

1. Department of Chemistry, Indian Institute of Technology Madras, Chennai, 600036 India.
  2. Centre for Atomistic Modelling and Materials Design, Indian Institute of Technology Madras, Chennai 600036, India.
  3. Centre for Quantum Information, Communication, and Computing, Indian Institute of Technology Madras, Chennai 600036, India.
  4. Centre for Molecular Materials and Functions, Indian Institute of Technology Madras, Chennai 600036, India.
  5. Centre for Computational and Data Science, Indian Institute of Technology Kharagpur, Kharagpur, West Bengal, 721302 India.
- \* yamijala@iitm.ac.in

Phonon spectra of cobalt anti-MXenes	2
Band structures and projected density of states of Co-anti-MXenes	3
Co-PDOS in pristine Co-anti-MXenes	4
CDD plots for the adsorption of Li/Na/K on various Co-anti-MXenes	6
Optimized structures of maximally lithiated Co-anti-MXenes	7
Optimized structures of maximally sodiated Co-anti-MXenes	8
Optimized structures of maximally potassiated Co-anti-MXenes	8
Thermal stability of maximally sodiated structures	9
ELF plots of maximally lithiated Co-anti-MXenes	10
ELF plots of maximally potassiated Co-anti-MXenes	10
ELF plots of Co-anti-MXenes with two layers of K atoms	10
Expansion of the CoP bilayer after the intercalation of Li	11
Expansion of the CoS bilayer after the intercalation of Na	12
Variation in the bandstructure of the CoS with Hubbard U	13
Validation for the kinetic energy cutoff and the k-mesh	14

## Phonon spectra of cobalt anti-MXenes

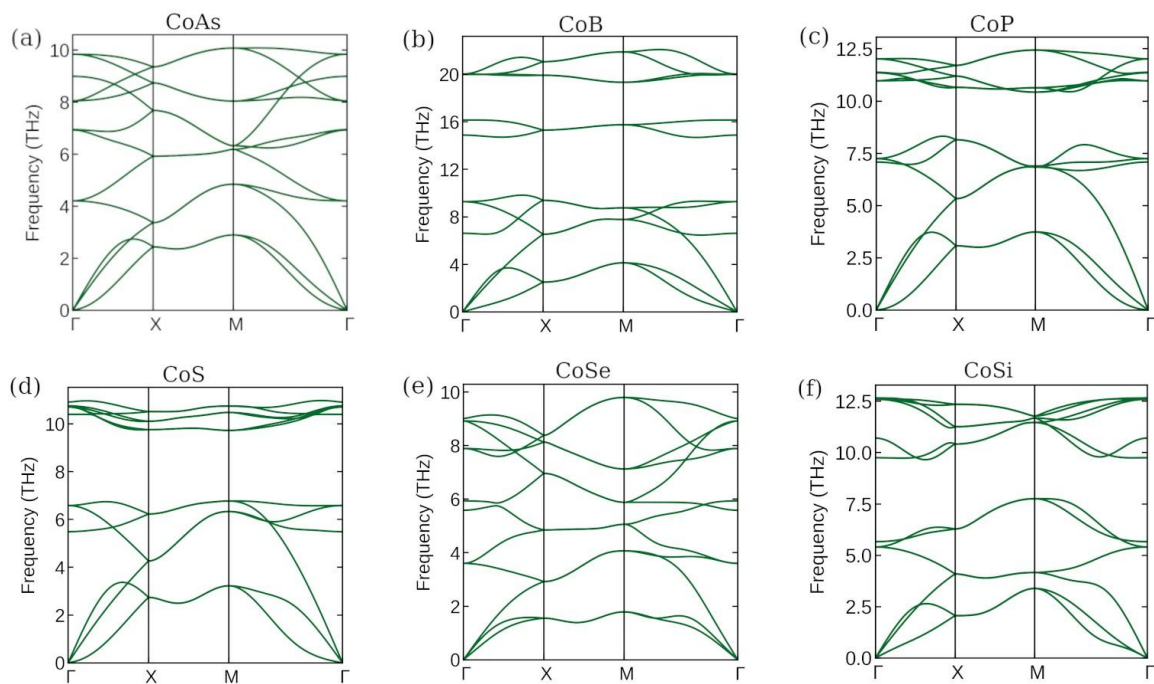


**Figure S1.** Phonon spectra of cobalt anti-MXenes. Positive frequencies indicate the dynamical stability of all systems.

## Band structures and projected density of states of Co-anti-MXenes

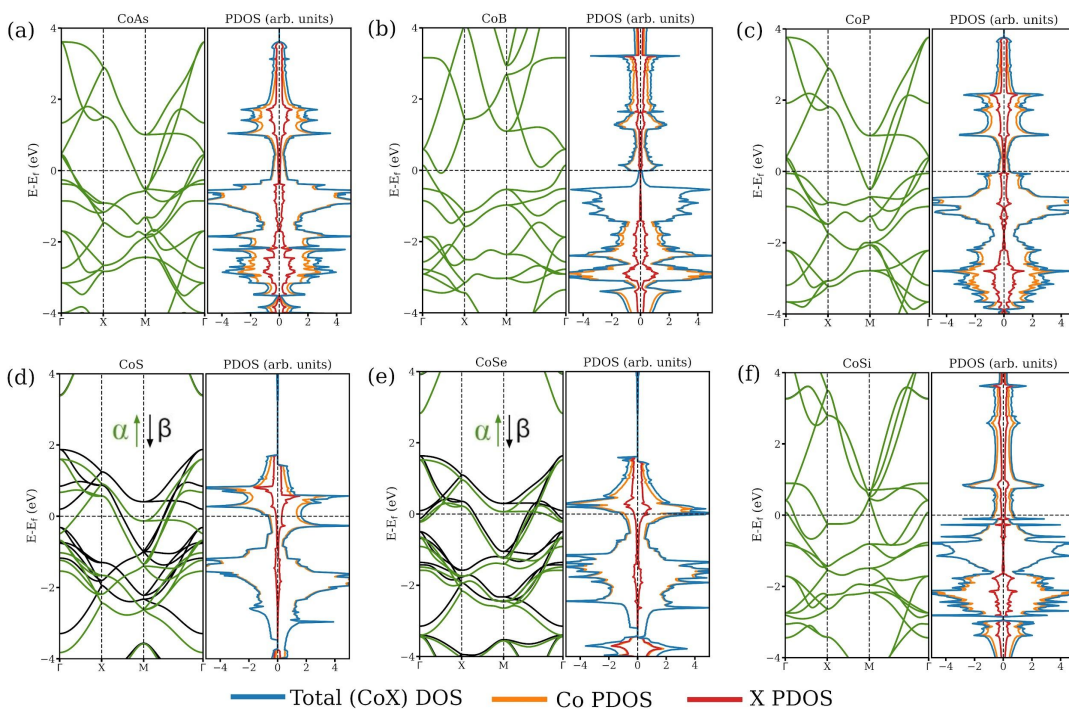


**Figure S2.** Band structure and projected density of states (PDOS) of (a) CoAs, (b) CoB, (c) CoP, (d) CoS, (e) CoSe, and (f) CoSi. All the anti-MXenes have a finite DOS near the Fermi level, indicating that they are metallic and have the potential to be used as electrodes. States across the Fermi level have a major contribution from the cobalt atoms, indicating their contribution to the metallicity. This figure is reproduced from reference 28 with permission.<sup>28</sup> (Copyright © 2022, American Chemical Society).

## Co-PDOS in pristine Co-anti-MXenes

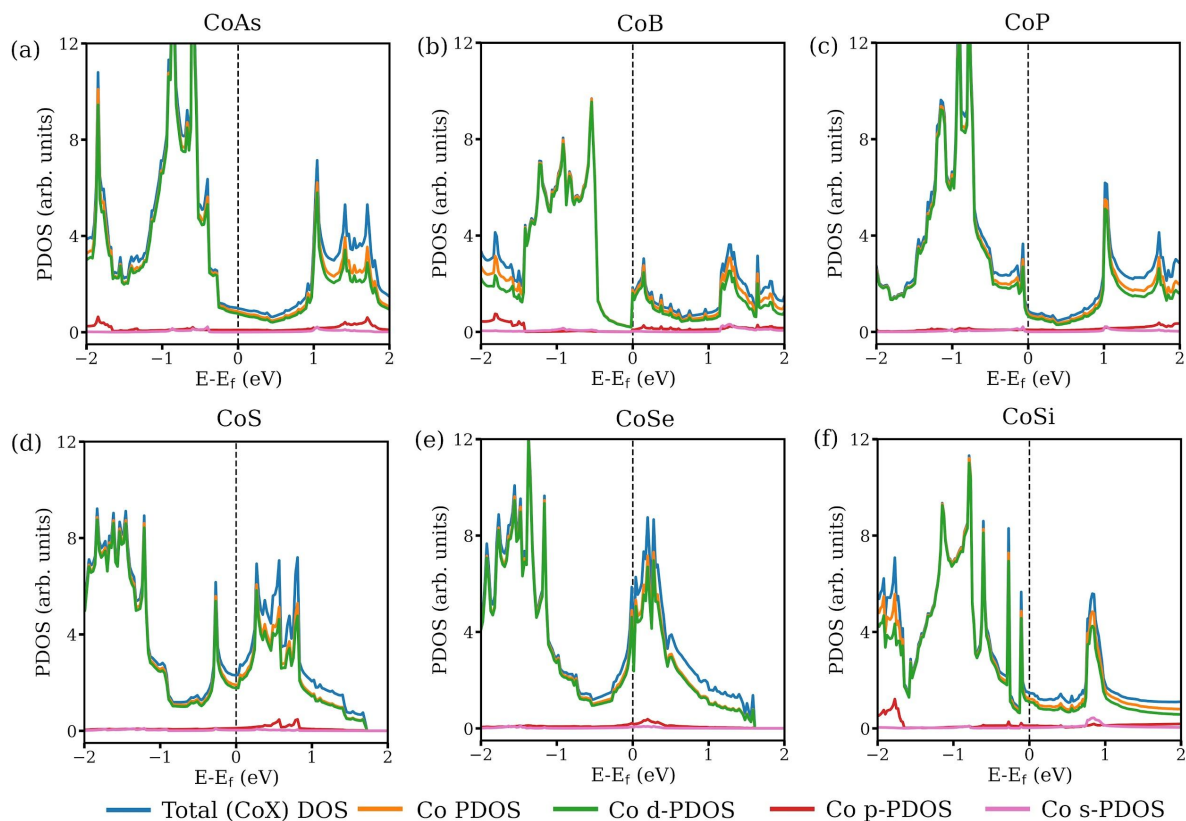


**Figure S3.** Projected density of states of ‘Co’ in pristine Co-anti-MXenes. The metallicity of Co-anti-MXenes is arising due to the d-orbitals of the Co. This figure is reproduced from reference 28 with permission.<sup>28</sup> (Copyright © 2022, American Chemical Society).

**Table S1.** Height (Å) of the Li/Na/K-atom from the CoX surface at the S1, S2, and S3 sites of a 3×3 supercell of Co-anti-MXenes.

System	Height (Å), Li			Height (Å), Na			Height (Å), K		
	S3	S1	S2	S3	S1	S2	S3	S1	S2
CoAs	<b>0.654</b>	1.507	2.388	<b>1.307</b>	2.041	2.703	<b>2.016</b>	2.524	3.050
CoB	<b>1.205</b>	1.627	2.081	<b>1.659</b>	2.018	2.386	<b>2.184</b>	2.450	2.736
CoP	<b>0.835</b>	1.553	2.323	<b>1.437</b>	2.045	2.646	<b>2.044</b>	2.500	2.989
CoS	<b>0.731</b>	1.385	2.187	<b>1.279</b>	1.885	2.543	<b>1.860</b>	2.359	2.874
CoSe	<b>0.530</b>	1.415	2.330	<b>1.307</b>	2.088	2.722	<b>2.223</b>	2.473	3.025
CoSi	<b>0.781</b>	1.578	2.411	<b>1.341</b>	2.018	2.718	<b>2.009</b>	2.517	3.029

**Table S2.** Bader charges on the alkali metal atom at various adsorption sites.

System	Charges, Li			Charges, Na			Charges, K		
	S3	S1	S2	S3	S1	S2	S3	S1	S2
CoAs	<b>0.856</b>	0.870	0.903	<b>0.818</b>	0.832	0.825	<b>0.833</b>	0.857	0.873
CoB	<b>0.874</b>	0.889	0.904	<b>0.829</b>	0.849	0.867	<b>0.856</b>	0.871	0.884
CoP	<b>0.866</b>	0.876	0.907	<b>0.832</b>	0.840	0.836	<b>0.843</b>	0.866	0.878
CoS	<b>0.872</b>	0.878	0.910	<b>0.849</b>	0.861	0.854	<b>0.855</b>	0.881	0.906
CoSe	<b>0.846</b>	0.862	0.877	<b>0.812</b>	0.779	0.693	<b>0.823</b>	0.844	0.836
CoSi	<b>0.851</b>	0.867	0.889	<b>0.797</b>	0.810	0.791	<b>0.818</b>	0.847	0.867

**Table S3.** Mulliken and Löwdin charges on the alkali metal atoms at the S3 adsorption sites.

Systems	Charges, Li		Charges, Na		Charges, K	
	Löwdin	Mulliken	Löwdin	Mulliken	Löwdin	Mulliken
CoAs	0.86	1.20	0.86	1.08	0.90	1.03
CoB	0.93	1.20	0.93	1.08	0.97	1.02
CoP	0.86	1.18	0.86	1.08	0.91	1.04
CoS	0.89	1.20	0.90	1.12	0.94	1.05
CoSe	0.81	1.09	0.76	0.89	0.84	0.92
CoSi	0.87	1.20	0.88	1.12	0.94	1.08

CDD plots for the adsorption of Li/Na/K on various Co-anti-MXenes

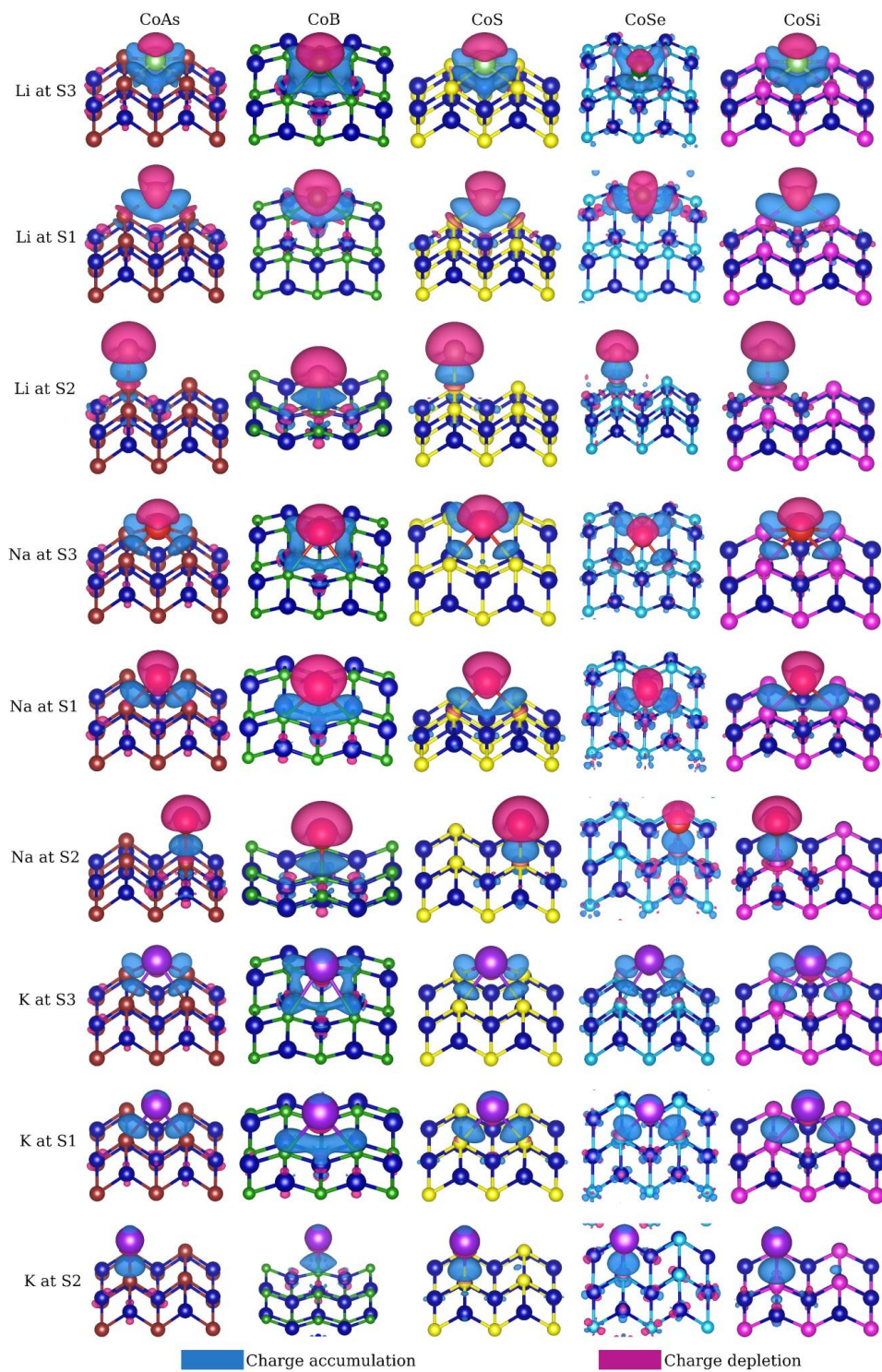


**Figure S4.** Charge density difference plots for the adsorption of Li/Na/K at the S1, S2, and S3 sites of Co- anti-MXenes. See the main text for calculation details and for the interpretation of the plots.



Optimized structures of maximally lithiated Co-anti-MXenes

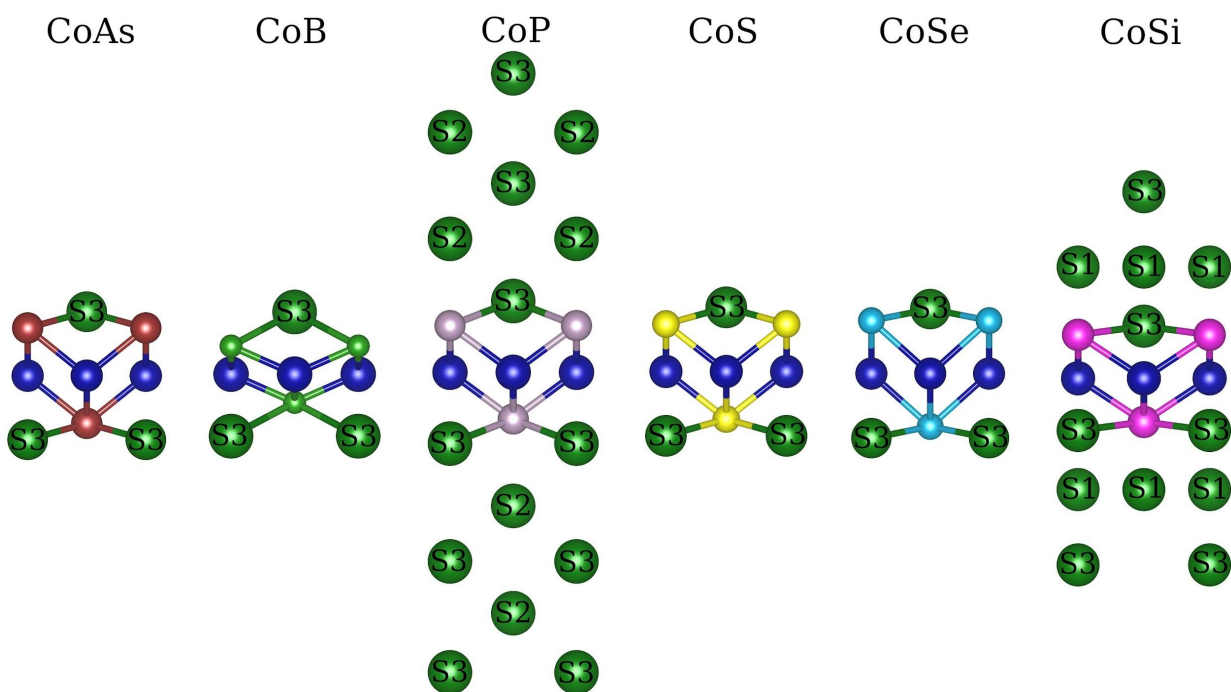


**Figure S5.** Optimized structures of various Co-anti-MXenes after the adsorption of a maximum number of lithium atoms. The molecular formulas of the maximally lithiated Co-anti-MXenes are  $\text{LiCoAs}$ ,  $\text{LiCoB}$ ,  $\text{Li}_5\text{CoP}$ ,  $\text{LiCoS}$ ,  $\text{LiCoSe}$ , and  $\text{Li}_4\text{CoSi}$ , respectively.

Optimized structures of maximally sodiated Co-anti-MXenes

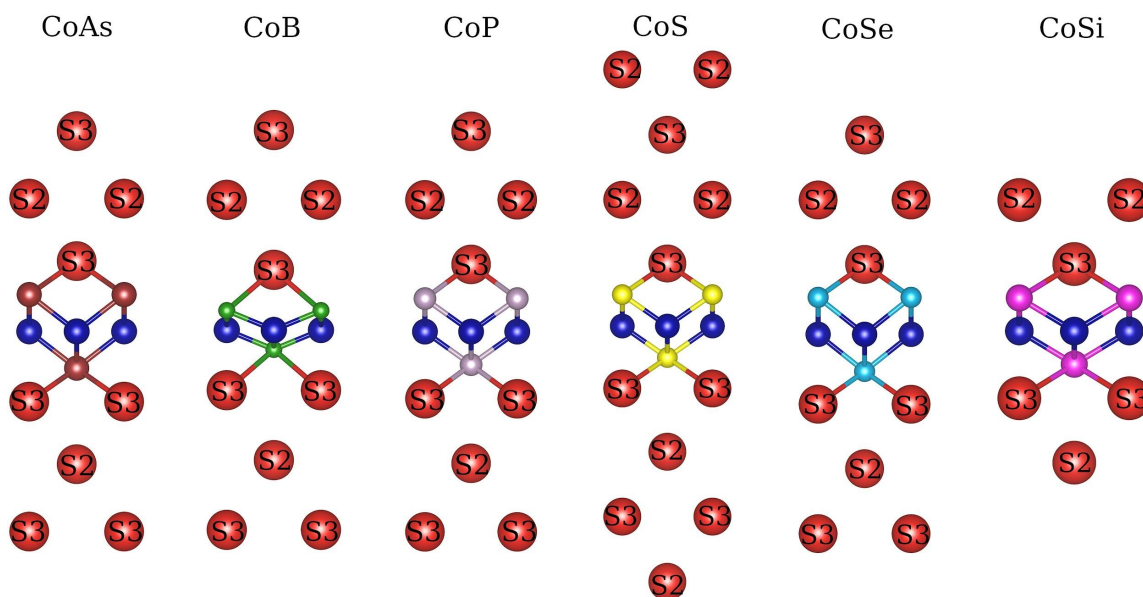


**Figure S6.** Optimized structures of various Co-anti-MXenes after the adsorption of a maximum number of sodium atoms. The molecular formulas of the maximally sodiated Co-anti-MXenes are  $\text{Na}_3\text{CoAs}$ ,  $\text{Na}_3\text{CoB}$ ,  $\text{Na}_3\text{CoP}$ ,  $\text{Na}_4\text{CoS}$ ,  $\text{Na}_3\text{CoSe}$ , and  $\text{Na}_2\text{CoSi}$ . This figure is reproduced from reference 28 with permission.<sup>28</sup> (Copyright © 2022, American Chemical Society).

Optimized structures of maximally potassiated Co-anti-MXenes

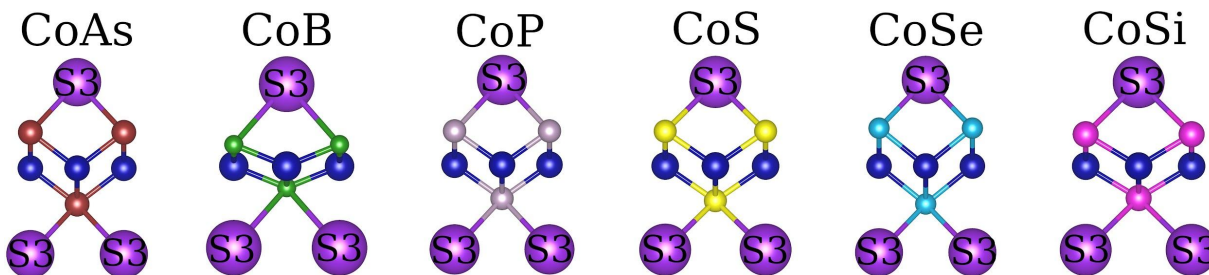


**Figure S7.** Optimized structures of various Co-anti-MXenes after the adsorption of a maximum number of potassium atoms. The molecular formula for all the maximally potassiated Co-anti-MXenes is the same:  $\text{KCoX}$  ( $X = \text{As}, \text{B}, \text{P}, \text{S}, \text{Se}, \text{and Si}$ ).



## Thermal stability of maximally sodiated structures

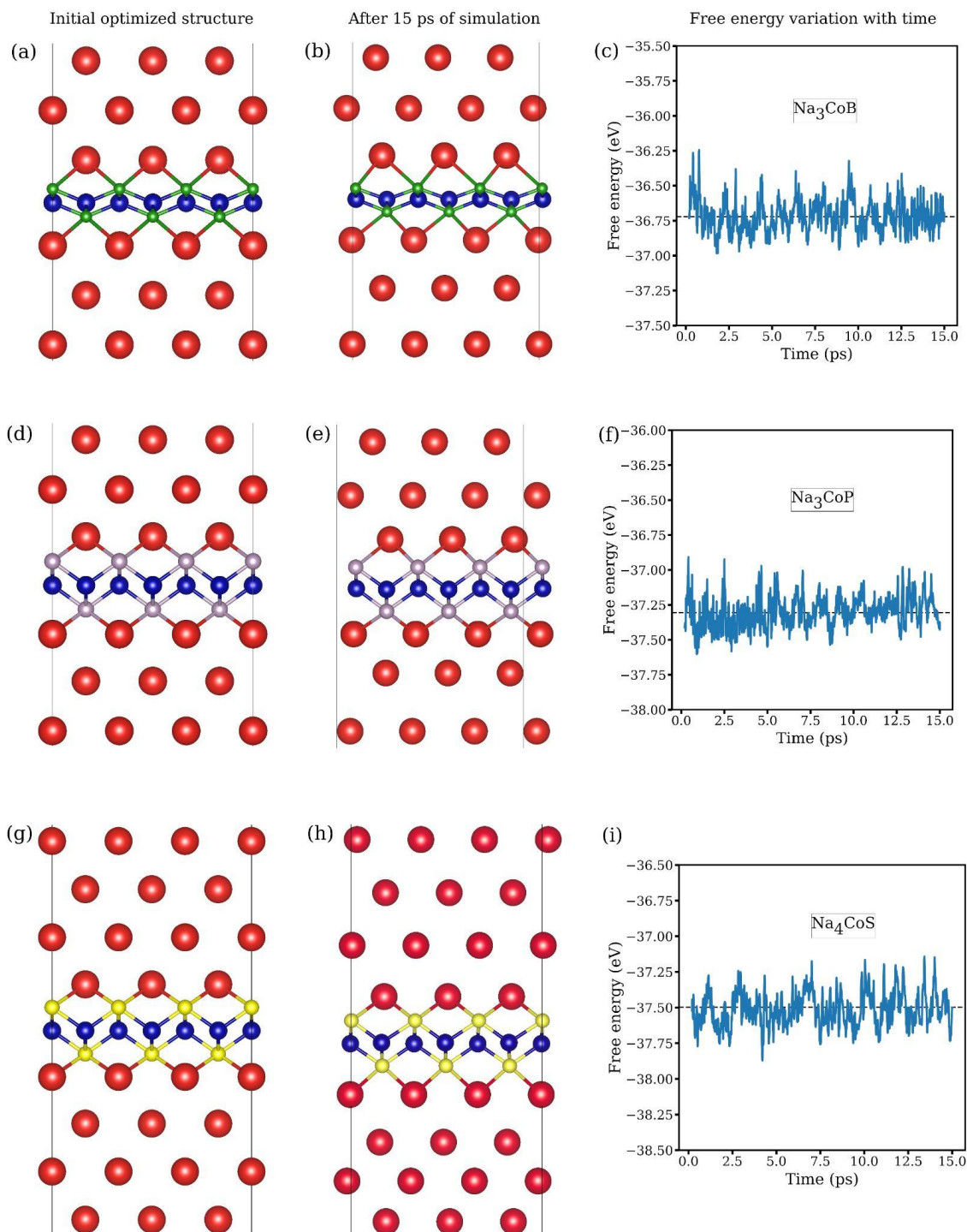


**Figure S8.** (a), (d), and (g) depict the optimized structures of  $\text{Na}_3\text{CoB}$ ,  $\text{Na}_3\text{CoP}$ , and  $\text{Na}_4\text{CoS}$  systems, respectively, at the 0<sup>th</sup> ps of the NVT simulation. (b), (e) and (h) depict the corresponding structures after a 15 ps NVT simulation. (c), (f) and (i) show the fluctuations in the free energy of  $\text{Na}_3\text{CoB}$ ,  $\text{Na}_3\text{CoP}$ , and  $\text{Na}_4\text{CoS}$  during the 15 ps NVT simulation (at 300 K). This figure is reproduced from reference 28 with permission.<sup>28</sup> (Copyright © 2022, American Chemical Society).

ELF plots of maximally lithiated Co-anti-MXenes

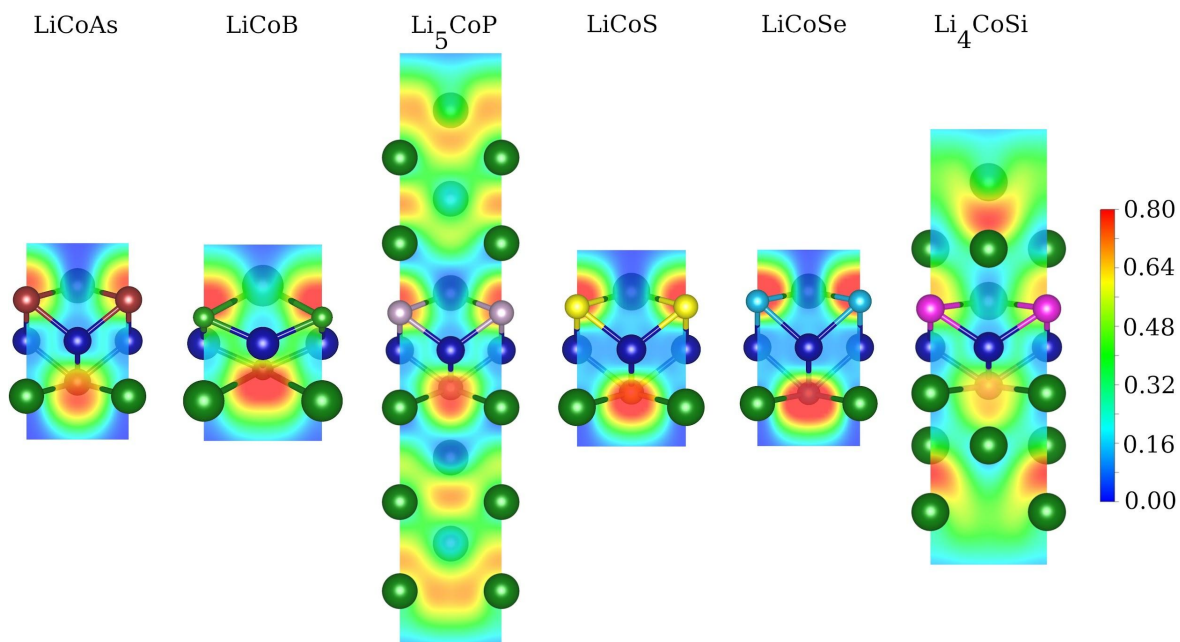


**Figure S9.** ELF plots of maximally lithiated Co-anti-MXenes. Plots are projected along the (010) plane.

ELF plots of maximally potassiated Co-anti-MXenes

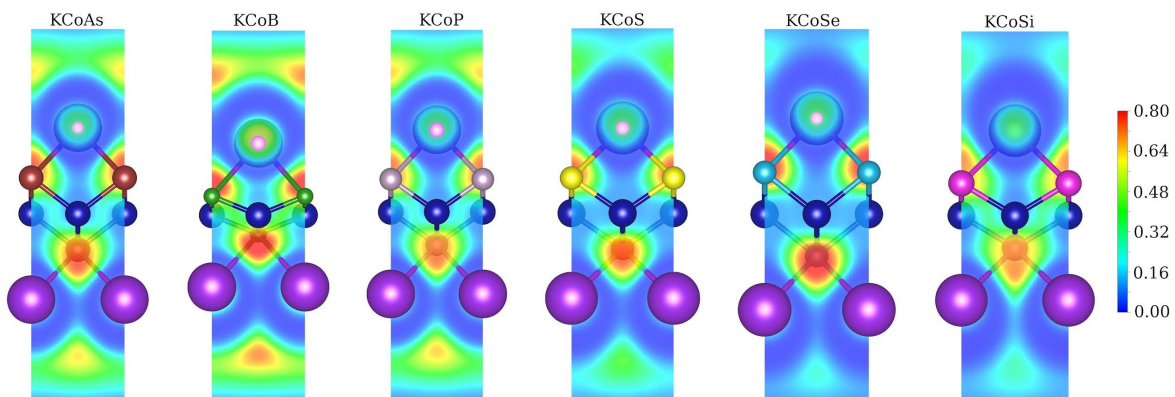


**Figure S10.** ELF plots of maximally potassiated Co-anti-MXenes. Plots are projected along the (010) plane.

ELF plots of Co-anti-MXenes with two layers of K atoms

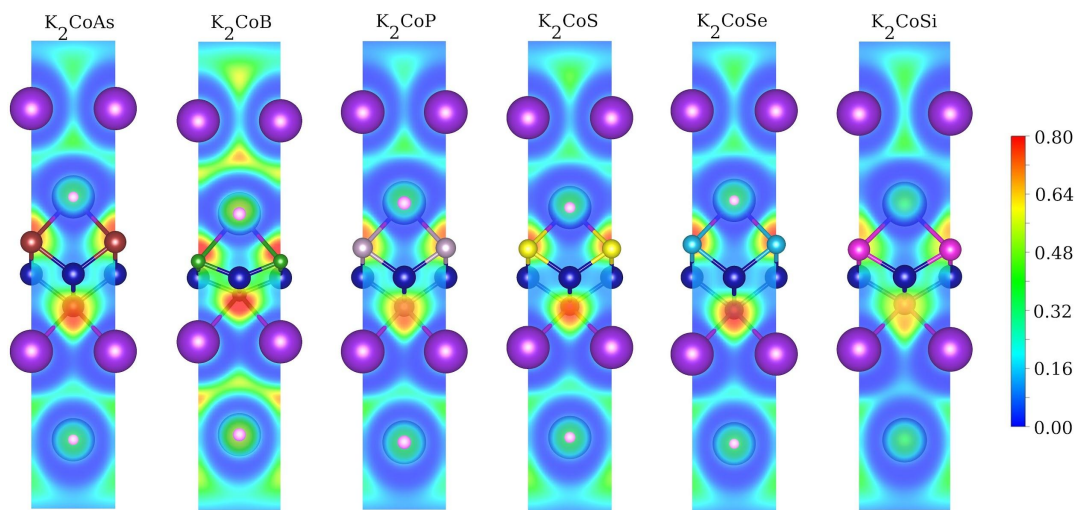


**Figure S11.** ELF plots of Co-anti-MXenes with two layers of K atoms (the maximally potassiated structures have only one layer of potassium atoms). Plots are projected along the (010) plane.

Expansion of the CoP bilayer after the intercalation of Li

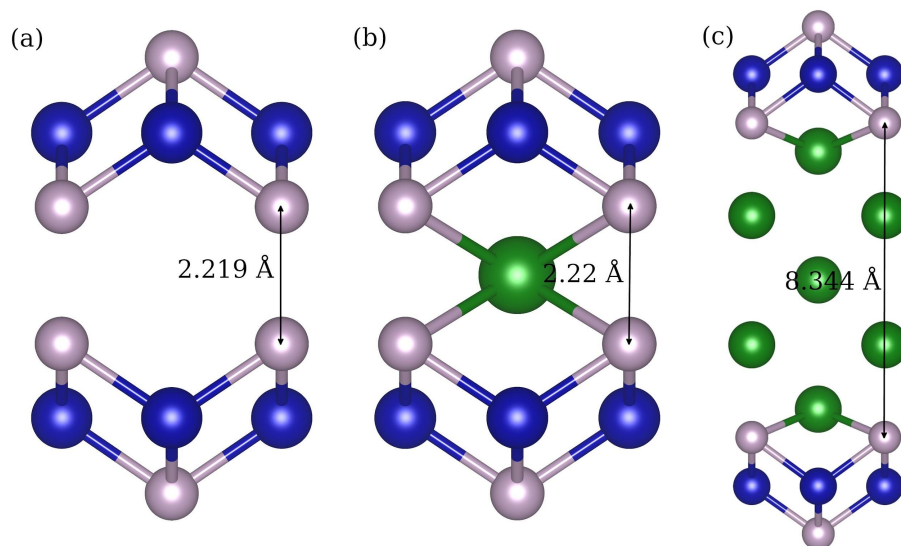


**Figure S12.** Optimized structures of (a) pristine CoP bilayer, (b) CoP bilayer with one layer of lithium atoms, and (c) CoP bilayer with five layers of Li atoms, respectively. The interlayer spacings between the CoP layers in these structures are 2.219 Å, 2.22 Å, and 8.344 Å, respectively.

Expansion of the CoS bilayer after the intercalation of Na

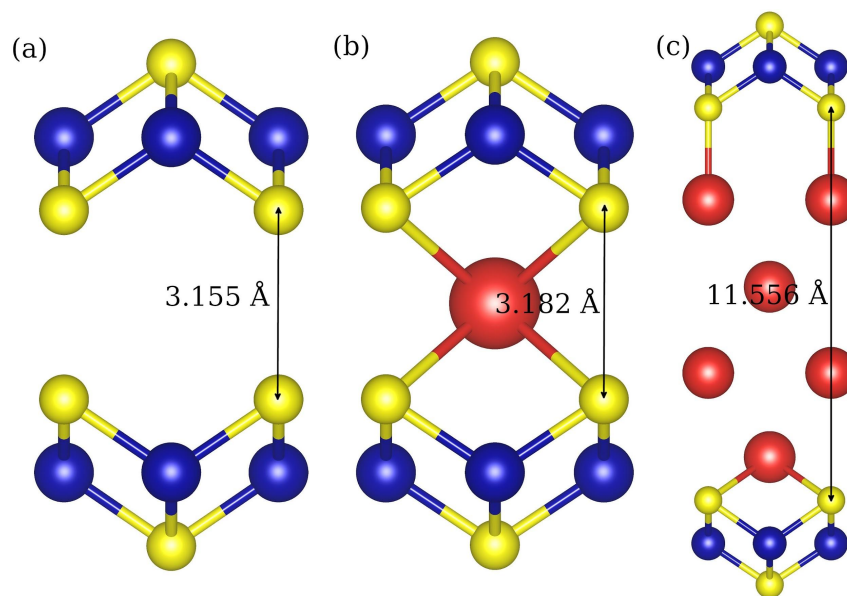


**Figure S13.** Optimized structures of (a) pristine CoS bilayer, (b) CoS bilayer with one layer of sodium atoms, and (c) CoS bilayer with four layers of Na atoms, respectively. The calculated interlayer spacings between the CoS layers in these structures are 3.155 Å, 3.182 Å, and 11.556 Å, respectively. This figure is reproduced from reference 28 with permission.<sup>28</sup> (Copyright © 2022, American Chemical Society).



Variation in the bandstructure of the CoS with Hubbard U

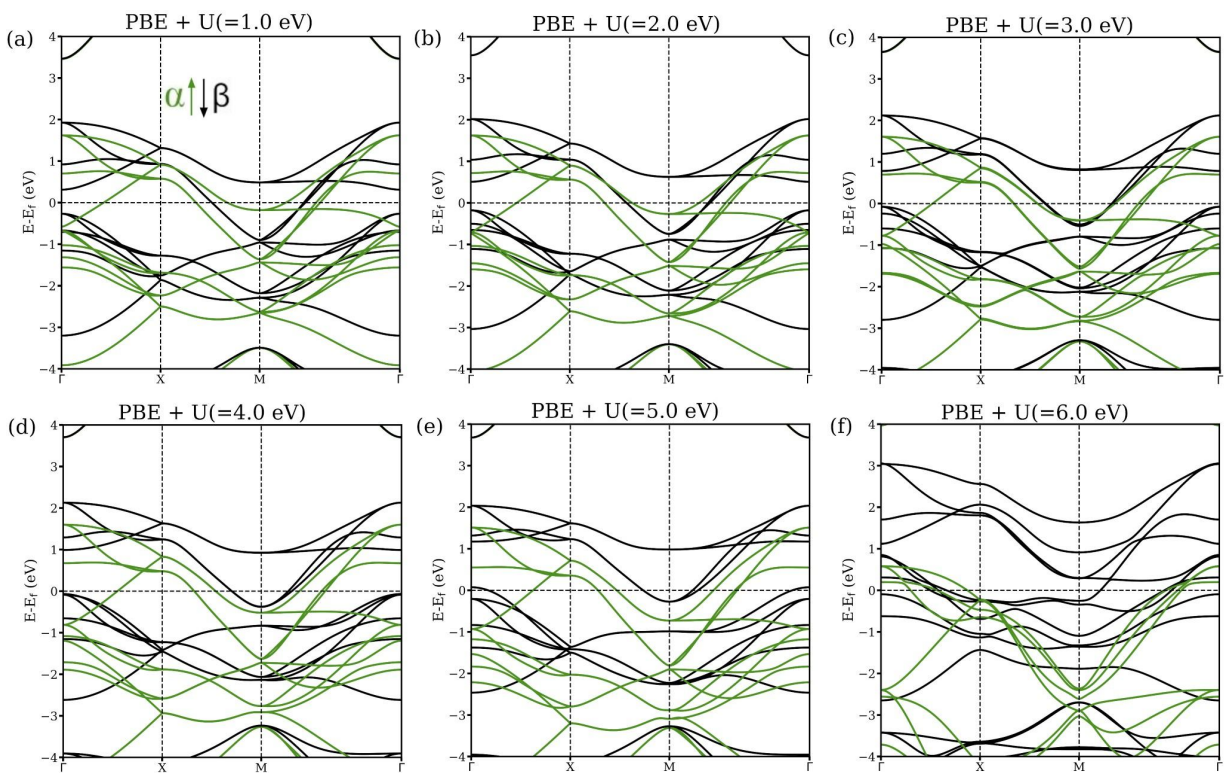


**Figure S14.** Computed bandstructures of the CoS system for both  $\alpha$  and  $\beta$ -spin channels at various U values ( $1\text{eV} \leq U \leq 6\text{eV}$ ). The corresponding U values are provided in the title of each panel.

## Validation for the kinetic energy cutoff and the k-mesh

**Table S4.** Variation in the total energy of a CoS unit cell with different kinetic energy cutoffs. All calculations are performed with a  $12 \times 12 \times 1$  k-mesh (only SCF optimization is performed)

ENCUT value (eV)	Total energy of the system (eV)	Energy difference (eV)
350	-24.845	–
400	-24.839	0.006
450	-24.837	0.002
500	-24.838	-0.001
550	-24.838	0.000
600	-24.838	0.000

**Table S5.** Variation in the total energy of a CoS unit cell with different k-mesh values. All calculations are performed with a 450 eV kinetic energy cutoff (only SCF optimization is performed).

K-mesh	Total energy of the system (eV)	Energy difference (eV)
$6 \times 6 \times 1$	-24.845	–
$8 \times 8 \times 1$	-24.830	0.015
$10 \times 10 \times 1$	-24.840	-0.010
$12 \times 12 \times 1$	-24.837	0.003
$14 \times 14 \times 1$	-24.836	0.001
$16 \times 16 \times 1$	-24.837	-0.001